

Chapter 2

Using Physical Chemistry to Differentiate Nicotinic from Cholinergic Agonists at the Nicotinic Acetylcholine Receptor

This chapter was reproduced in part with permission from Cashin et al, *Journal of the American Chemical Society* **127**, 350-356 (2005). Copyright 2005 American Chemical Society.

2.1 INTRODUCTION

Biological signaling pathways employ a vast array of integral membrane proteins that process and interpret the chemical, electrical, and mechanical signals that are delivered to cells. These proteins are the targets of most drugs of therapy and abuse, but structural insights are sparse because both x-ray crystallography and NMR spectroscopy are of limited applicability. Even when structural information is available, establishing the functional importance of particular structural features can be challenging. In contrast, chemistry-based methods hold great promise for producing high-precision structural and functional insights. Varying the drug or signaling molecule has been the approach of the pharmaceutical industry, producing a multitude of structure-activity relationships of considerable value. In recent years we have taken the reverse approach, in which we systematically vary the receptor and use functional assays to monitor changes in drug-receptor interactions.^{1,2} We show here that this physical chemistry approach to studying receptors can produce high-precision insights into drug-receptor interactions. In particular, we show that two agonists that interact with the same binding pocket of a receptor can make use of very different noncovalent interactions to achieve the same result.

The ligand gated ion channels (LGIC) are among the molecules of memory, thought, and sensory perception and are the targets for treatments of Alzheimer's disease, Parkinson's disease, schizophrenia, stroke, learning deficits, and drug addiction.^{3,4} The binding of small molecule neurotransmitters induces a structural change, opening a pore in a channel that allows the passage of ions across the cell membrane. Here we examine the agonist-binding site of the nicotinic acetylcholine receptor (nAChR), the prototype of the Cys-loop family of LGIC, which also includes γ -aminobutyric acid, glycine, and

serotonin receptors. The embryonic muscle nAChR is a cylindrical transmembrane protein⁵ composed of five subunits ($\alpha 1$)₂, $\beta 1$, γ , and δ (**Figure 2.1A**). Early biochemical studies identified two agonist-binding sites localized to the α/δ and α/γ interfaces.⁶⁻⁸ The crystal structure of the acetylcholine-binding protein (AChBP),⁹ a soluble protein homologous to the agonist-binding site of the nAChR, revealed the binding sites to be defined by a box of conserved aromatic residues.

A cationic center is contained in nearly all nAChR agonists, including acetylcholine (ACh) and (-) nicotine. A common strategy for the recognition of cations by biological molecules is the cation- π interaction, the stabilizing interaction between a cation and the electron-rich face of an aromatic ring.¹⁰⁻¹² Studies of the muscle-type nAChR using unnatural amino acid mutagenesis showed that a key tryptophan, Trp $\alpha 149$, makes a potent cation- π interaction with ACh in the agonist-binding site.¹³ Interestingly nicotine, binding in the same pocket of the muscle-type nAChR, does not make a strong cation- π interaction.¹⁴ These findings suggested that agonists of the nAChR could fall into two classes, which for present purposes we will term “cholinergic,” binding like ACh, and “nicotinic,” binding like nicotine.

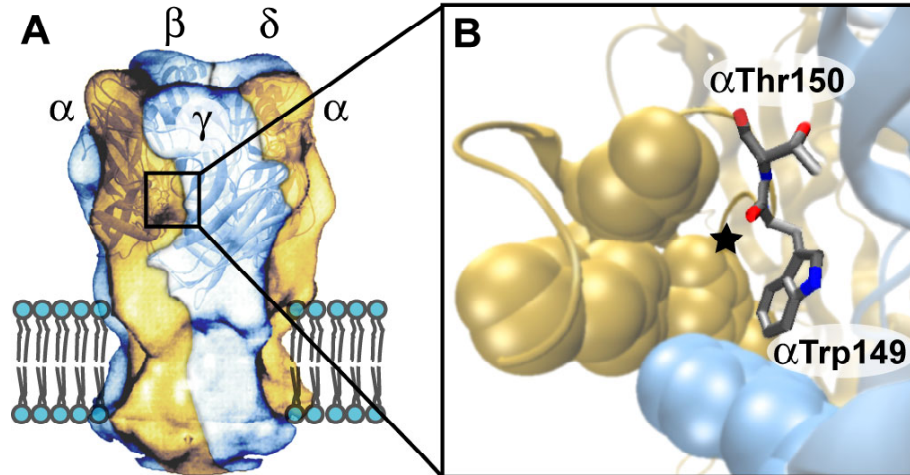


Figure 2.1. Images of the nAChR. (A) The overall layout of the muscle receptor, indicating the arrangement of five subunits around a central pore. The receptor electron density from cryo-electron microscopy⁵ is shown superimposed over a ribbon diagram of AChBP⁹, which corresponds to the extracellular domain of the receptor. (B) The agonist binding site from AChBP with muscle-type nAChR numbering. Aromatic residues lining the binding pocket are shown as space-filling models. Residues and ribbons from the α subunit are gold; those from the δ subunit are blue. The star marks the backbone carbonyl that participates in a hydrogen bond with agonists.

Several modeling studies based on the original structure of AChBP suggested a hydrogen-bonding interaction from the $N^+ - H$ of nicotine to the backbone carbonyl of Trp $\alpha 149$.^{15,16} This carbonyl is denoted by a star in **Figure 2.1**. ACh cannot make a hydrogen bond of this sort. Thus, this hydrogen bond could be a second discriminator between ACh and nicotine (the first being the cation- π interaction with Trp $\alpha 149$). While this work was nearing completion, Sixma and co-workers reported the crystal structure of AChBP in the presence of bound nicotine,¹⁷ confirming the proposed hydrogen bond between nicotine and the backbone carbonyl of Trp $\alpha 149$ at the agonist-binding site. We note, however, that AChBP is not a neuroreceptor, and that it shares only 20-24% sequence identity with nAChR α subunits. In addition, the crystal structure of AChBP most likely represents the desensitized state of the receptor. Thus, the *functional*

significance of structural insights gained from AChBP remains to be determined, and the present paper addresses this issue.

One challenge in studying the activity of nicotine at the nAChR is that nicotine has low agonist potency at the muscle receptor subtype.¹⁸ Nicotine is a more potent agonist at some neuronal nAChR subtypes.¹⁹ As such, the present study also examines epibatidine, a very potent agonist at both muscle and neuronal-type nAChRs.^{19,20} Epibatidine, while structurally similar to nicotine, has a potency comparable to ACh.^{21, 22} Therefore, epibatidine perhaps serves as a more meaningful probe of “nicotinic” interactions at the muscle-type nAChR (**Figure 2.2**).

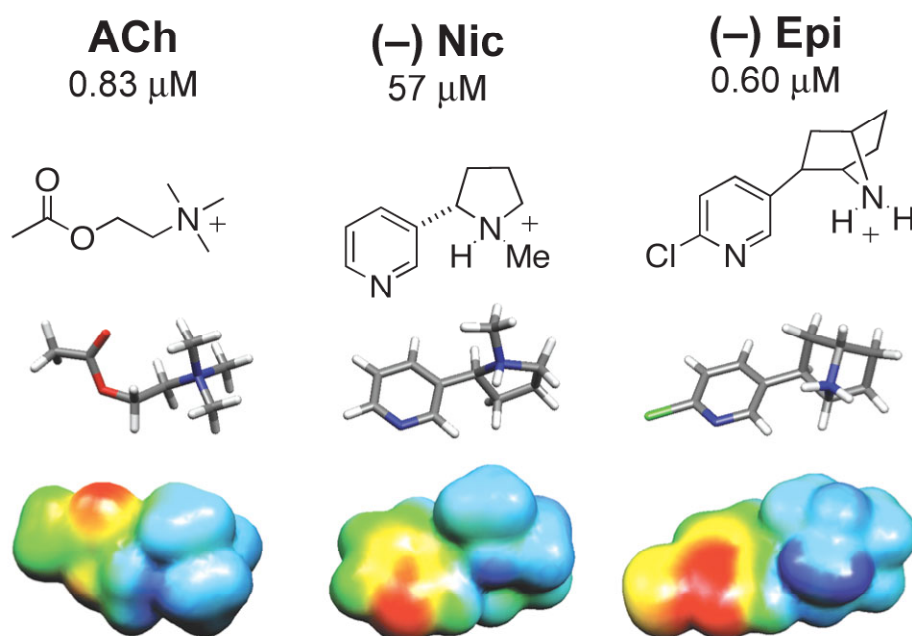


Figure 2.2. nAChR Agonists Examined in This Study. Shown are EC_{50} values for activation of the wild-type nAChR and calculated agonist geometries. HF/6-31G electrostatic surfaces calculated using Molekel contrast the focused N^+-H positive charge on nicotine and epibatidine with the diffuse ACh ammonium charge. Electrostatic surfaces correspond to an energy range of +10 to +130 kcal/mol, where blue is highly positive and red is less positive. Note that (\pm) epibatidine was used to obtain EC_{50} values.

The goals of this study were thus twofold. First, we wished to evaluate the significance of the apparent hydrogen bond between nicotine and the backbone carbonyl of Trp α 149. Second, we wished to evaluate the factors that render epibatidine almost 100-fold more potent than nicotine, despite the clear structural similarity of the two. The site-specific *in vivo* nonsense suppression methodology for unnatural amino acid incorporation² has been exploited to evaluate these two issues. Studies employing fluorinated Trp derivatives at α 149 reveal that epibatidine binds with a potent cation- π interaction similar to that of ACh. In addition, we establish the functional significance of the interaction with the backbone carbonyl at Trp α 149 with both nicotine and epibatidine by weakening the hydrogen bond ability of the backbone carbonyl through an appropriate backbone amide-to-ester mutation. Modeling based on these data suggests precise interactions that differentiate the three agonists.

2.2 MATERIALS AND METHODS

Synthesis of α -hydroxy threonine (Tah, 2R, 3S-dihydroxy-butanoic acid)²³

L-Threonine (2.2 g, 18.5 mmol), suspended in 5 ml of water at -5 °C, was treated simultaneously with a solution of 1.38 g NaNO₂ (20 mmol) in 2 ml of water and 557 μ l of concentrated H₂SO₄ (10 mmol) in 1.5 ml H₂O. The two solutions were added slowly while stirring so that the temperature remained between 0 °C and 5 °C. The reaction turned yellow upon addition. The solution was then stirred overnight at room temperature. The reaction mixture was concentrated, the mixture was treated with 3 ml of EtOH, and the salts were filtered. The solution was concentrated. The material was dry loaded onto a flash silica gel column and run in 1:1 hexanes/ethyl acetate with 1%

acetic acid to give 730 mg (38 %) of hydroxythreonine: ^1H NMR (D_2O) δ 1.17 (d, 3 H, $J = 6$ Hz), 4.1 (m, 2H); ^{13}C NMR 18.2, 68.4, 74.2, 176.0: Electrospray MS Calcd for $\text{C}_4\text{H}_8\text{O}_4$ minus H: 119.1. Found m/z : 119.0.

Synthesis of Tah Cyanomethyl Ester (2*R*, 3*S*-dihydroxy-butanoate cyanomethyl ester)²⁴

The hydroxy acid (385 mg, 3.21 mmol) was dissolved in 5.1 ml of ClCH_2CN (80.1 mmol) and 1.2 ml Et_3N (8.44 mmol). Upon stirring under Ar for 30 min, the solution turned yellow. A gradient flash silica gel column from 20% to 80% ethyl acetate/hexanes was run, and the isolated product was dried on vacuum to yield 50.9 mg (10%) of hydroxythreonine cyanomethyl ester: ^1H NMR (D_2O) δ 1.27 (d, 3H, $J = 6$ Hz), 4.22 (m, 1H), 4.34 (d, 1H, $J = 3$ Hz), 5.01 (s, 2H), ^{13}C 18.2, 49.7, 68.4, 74.4, 115.5, 172.6; FAB MS Calcd for $\text{C}_6\text{H}_9\text{O}_4\text{N}$ plus H: 160.17. Found m/z : 160.03 (M+H), 75.02, 103.07.

Synthesis of dCA-Tah

Tah cyanomethyl ester (5.7 mg, 35.8 μmol) was dissolved in 250 μl dry DMF in a flame-dried 5 ml round bottom flask with a stir bar. The dinucleotide dCA (14.4 mg, 11.9 μmol) was added, and the reaction was stirred under Ar for 24 h. Upon completion of the reaction, the pure compound was obtained by preparative HPLC. Electrospray MS Calcd for $\text{C}_{23}\text{H}_{31}\text{N}_8\text{O}_{16}\text{P}_2$ minus H: 736.13. Found m/z (M-H): 737.4.

Western Blot Analysis

In vitro transcription was performed using Promega rabbit reticulocyte lysate translation system as reported previously.^{25,26} Untreated and base (NH₄OH) treated samples were prepared to detect base hydrolysis of backbone esters as previously described in detail.²⁶

Electrophysiology

Stage VI oocytes of *Xenopus laevis* were employed. Oocyte recordings were made 24 to 48 h post injection in two-electrode voltage clamp mode using the OpusXpressTM 6000A (Axon Instruments, Union City, California). Oocytes were superfused with Ca²⁺-free ND96 solution at flow rates of 1 ml/min, 4 ml/min during drug application and 3 ml/min during wash. Holding potentials were -60 mV. Data were sampled at 125 Hz and filtered at 50 Hz. Drug applications were 15 s in duration. Agonists were purchased from Sigma/Aldrich/RBI: (-) nicotine tartrate, acetylcholine chloride, and (±) epibatidine dihydrochloride. Epibatidine was also purchased from Tocris as (±) epibatidine. All drugs were prepared in sterile ddi water for dilution into calcium-free ND96. Dose-response data were obtained for a minimum of 10 concentrations of agonists and for a minimum of 7 cells. Dose-response relations were fitted to the Hill equation to determine EC₅₀ and Hill coefficient. EC₅₀s for individual oocytes were averaged to obtain the reported values.

Unnatural Amino Acid Suppression

Synthetic amino acids and α -hydroxy acids were conjugated to the dinucleotide dCA and ligated to truncated 74 nt tRNA as previously described.^{24,27} Deprotection of

aminoacyl tRNA was carried out by photolysis immediately prior to co-injection with mRNA, as described.^{27, 28} Typically, 25 ng of tRNA were injected per oocyte along with mRNA in a total volume of 50 nl/cell. mRNA was prepared by *in vitro* runoff transcription using the Ambion (Austin, TX) T7 mMessage mMachine kit. Mutation to the *amber* stop codon at the site of interest was accomplished by standard means and was verified by sequencing through both strands. For nAChR suppression, a total of 4.0 ng of mRNA was injected in the subunit ratio of 10:1:1:1 α : β : γ : δ . In all cases, the β subunit contained a Leu9'Ser mutation, as discussed below. Mouse muscle embryonic nAChR in the pAMV vector was used, as reported previously. In addition, the α subunits contain an HA epitope in the M3-M4 cytoplasmic loop for biochemical western blot studies (**Figure 2.4**). Control experiments show a negligible effect of this epitope on EC₅₀. As a negative control for suppression, truncated 74 nt or truncated tRNA ligated to dCA was co-injected with mRNA in the same manner as fully charged tRNA. At the positions studied here, no current was ever observed from these negative controls. The positive control for suppression involved wild-type recovery by co-injection with 74 nt tRNA ligated to dCA-Thr or dCA-Trp. In all cases, the dose-response data were indistinguishable from injection of wild-type mRNA alone.

Computation

This study was performed in collaboration with E. James Petersson, who conducted the computation studies. Acetylcholine, (-) nicotine, (+) epibatidine, (-) epibatidine, 3-(1H-Indol-3-yl)-*N*-methyl-propionamide, 3-(1H-Indol-3-yl)-*O*-methyl-propionate, and the hydrogen-bonded complexes shown in **Figure 2.5** were optimized at the HF/6-31G

level of theory. For the acetylcholine, (-) nicotine, and (-) epibatidine complexes, the starting coordinates of the ligand and Trp 147 ($\alpha 7$ numbering) were taken from the docked structures of Changeux and co-workers available at <http://www.pasteur.fr/recherche/banques/LGIC/LGIC.html>. The optimized geometries were fully characterized as minima by frequency analysis, and are reported elsewhere.²⁹ Energies were calculated at the HF/6-31G level. Basis set superposition error (BSSE) corrections were determined in the gas phase at the HF/6-31G level, using the counterpoise correction method of Boys and Bernardi.³⁰ Zero point energy (ZPE) corrections were included by scaling the ZPE correction given in the HF/6-31G level frequency calculation by the factor of 0.9135 given by Foresman and Frisch.³¹ All calculations were carried out with the Gaussian 98 program.³² Binding energies were determined by comparing the BSSE- and ZPE-corrected energies of the separately optimized ligand and tryptophan analog to the energy of the complex. Solvent effects were added to the gas phase-optimized structures using the polarizable continuum model (PCM) self-consistent reaction field of Tomassi and co-workers³³ with $\epsilon(\text{THF}) = 7.6$, $\epsilon(\text{EtOH}) = 24.3$, and $\epsilon(\text{H}_2\text{O}) = 78.5$.

Electrostatic potential surfaces were created with Molekel, available at www.cscs.ch/molekel/.³⁴ The electrostatic potential for each structure was mapped onto a total electron density surface contour at $0.002 \text{ e}/\text{\AA}^3$. These surfaces were color-coded so that red signifies a value less than or equal to the minimum in positive potential and blue signifies a value greater than or equal to the maximum in positive potential.

2.3 RESULTS

Unnatural amino acids were incorporated into the nAChR using *in vivo* nonsense suppression methods, and mutant receptors were evaluated electrophysiologically.² The structures and electrostatic potential surfaces of the agonists are presented in **Figure 2.2**. For these cationic agonists, the surface is positive everywhere; red simply represents relatively less positive, and blue relatively more positive. The structures and the electrostatic potential surfaces of the fluorinated tryptophan unnatural amino acids are shown in **Figure 2.3**. The calculated gas phase cation- π binding energies with a Na⁺ are indicated.¹³

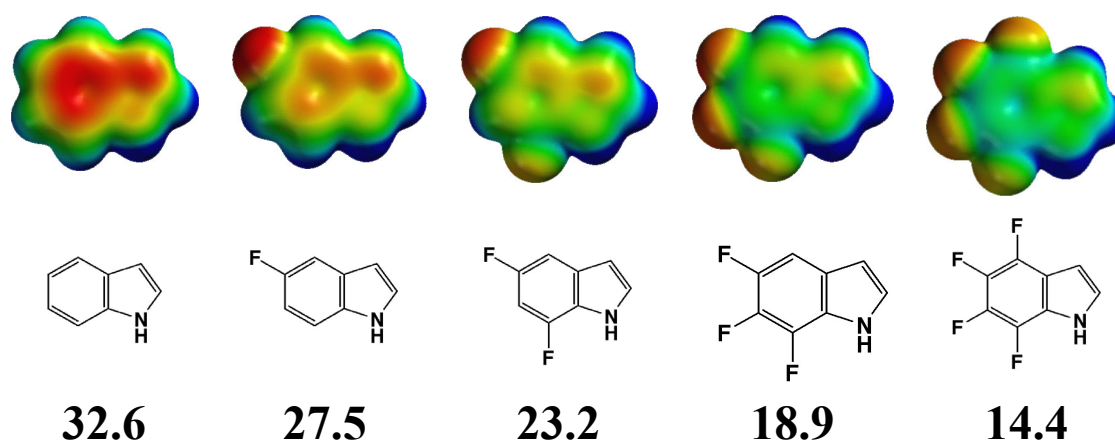


Figure 2.3. Fluorinated Tryptophan Series.¹³ Electrostatic potential surfaces are shown on a colorimetric scale from -25 (red) to $+25$ (blue) kcal/mol. Calculated gas phase Na⁺ binding energies are shown.

In studies of weak agonists and/or receptors with diminished binding capability, it is necessary to introduce another mutation that independently decreases EC₅₀. We accomplished this via a Leu-to-Ser mutation in the β subunit at a site known as 9' in the M2 transmembrane region of the receptor.³⁵⁻³⁷ This M2- β 9' residue is almost 50 Å from the binding site, and previous work has shown that a Leu9'Ser mutation lowers the EC₅₀

by a factor of roughly 40 without altering trends in EC₅₀ values.^{14, 38} Measurements of EC₅₀ represent a functional assay; all mutant receptors reported here are fully functioning ligand gated ion channels. It is important to appreciate that the EC₅₀ value is not a binding constant, but a composite of equilibria for both binding and gating. As we have shown in previous studies of LGIC using the unnatural amino acid methodology,^{1,2,13,14,28,38-40} the trends observed in EC₅₀s resulting from subtle changes in a series of residues that define the agonist-binding site are assumed to occur due to variations in agonist binding events rather than significant variations influencing the gating processes.

Epibatidine Binds with a Potent Cation- π Interaction at Trp α 149

The possibility of a cation- π interaction between epibatidine and Trp α 149 was evaluated using our previously developed strategy, the incorporation of a series of fluorinated Trp derivatives (5-F-Trp, 5,7-F₂-Trp, 5,6,7-F₃-Trp, and 4,5,6,7-F₄-Trp). The EC₅₀ values for the wild-type and mutant receptors are shown in **Table 2.1**. Attempts to record dose-response relations from 4,5,6,7-F₄-Trp at α 149 were unsuccessful because this mutant required epibatidine concentrations above 100 μ M. At these concentrations epibatidine becomes an effective open channel blocker,²⁰ confounding efforts to obtain an accurate dose-response curve. A clear trend can be seen in the data of **Table 2.1**: each additional fluorine produces an increase in EC₅₀.

As in previous work, our measure for the cation- π binding ability of the fluorinated Trp derivatives is the calculated binding energy of a generic probe cation (Na⁺) to the corresponding substituted indole (**Figure 2.3**).^{13, 14, 39} This method provides a convenient way to express the clear trend in the dose-response data in a quantitative way. A

“fluorination plot” of the logarithmic ratio of the mutant EC_{50} to the wild-type EC_{50} versus the cation- π binding ability for Trp α 149 reveals a compelling linear relationship (Figure 2.4). These data demonstrate that the secondary ammonium group of epibatidine makes a cation- π interaction with Trp α 149 in the muscle-type nAChR.

Table 2.1. Mutations Testing Cation- π Interactions at α 149

	Trp	F-Trp	F ₂ -Trp	F ₃ -Trp
Epibatidine ^a	0.83 0.08 ^b	$\pm 4.8 \pm 0.1$	9.3 ± 0.5	18 ± 2
Cation- π ^c	32.6	27.5	23.3	18.9

^a EC_{50} (μ M) \pm standard error of the mean. Racemic epibatidine was used in these experiments. The receptor has a Leu9’Ser mutation in M2 of the β subunit.

^b Rescue of wild type by nonsense suppression.

^c Reference ¹³. Value reported is the negative of the calculated binding energy of a probe cation (Na^+) to the ring, in kcal/mol.

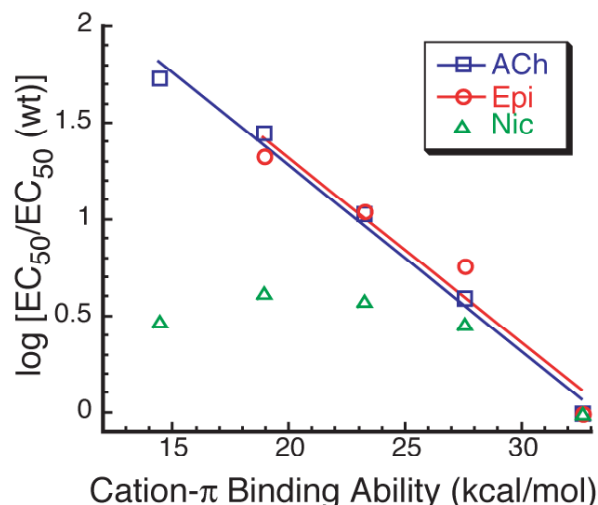


Figure 2.4. Fluorination Plot for nAChR Agonists. Epibatidine data from **Table 2.1**; ACh data from Reference ¹³, nicotine data from Reference ¹⁴. The $\log [EC_{50} / EC_{50} (wt)]$ versus calculated cation- π ability is plotted for the series of fluorinated Trp derivatives at Trp $\alpha 149$. ACh data fit the line $y = 3.21 - 0.096x$ and epibatidine data fit the line $y = 3.23 - 0.096x$. The correlation for ACh and epibatidine fits were $R = 0.99$ and $R = 0.98$, respectively. Note that because the data for each agonist are normalized to the EC_{50} of the wild-type receptor, all three agonists share the point for the wild-type receptor, with coordinates (32.6, 0).

***In vitro* Nonsense Suppression at $\alpha 150$**

Biochemical studies were conducted to confirm the presence of alpha hydroxyl-threonine at $\alpha 150$ in the mouse muscle nAChR. *In vitro* nonsense suppression in rabbit reticulocyte lysate was conducted by transcribing mRNA coding the $\alpha 150TAG$. The alpha construct contains an HA epitope (YPYDVPDYA) for protein visualization on a Western blot with antibodies against the HA sequence. Full-length protein was observed in lanes containing mRNA and Thr or Tah charged tRNA. No protein was observed in lanes containing mRNA only or mRNA with uncharged tRNA (labeled trunc tRNA in **Figure 2.5**).

Proteins containing Tah at $\alpha 150TAG$ contain an ester backbone and can be detected by treating the transcription products with concentrated base (NH_4OH). Ester backbones

are hydrolyzed by concentrated base and the cleavage product can be visualized on a western blot.^{24,26} **Figure 2.5** shows a western blot of nAChR α subunit suppressed with Thr and Tah. The arrow indicates the cleaved product, observed only in the Tah base-treated lanes. This figure verifies that Tah is incorporated into the protein.

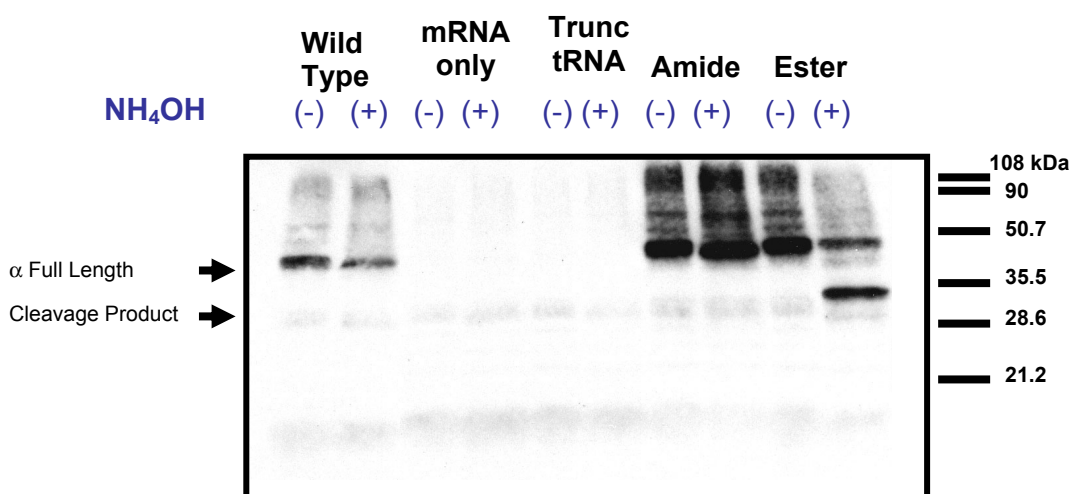


Figure 2.5. *In Vitro* Suppression at α 150. Protein contains an HA epitope. Samples were treated with NH_4OH base (+) or loaded as is (-). The full-length protein and base cleavage product are indicated.

Nicotine and Epibatidine Hydrogen Bond to the Carbonyl Oxygen of Trp α 149

The recently reported crystal structure of AChBP with nicotine bound indicated a hydrogen bond between the pyrrolidine $\text{N}^+\text{-H}$ of nicotine and the backbone carbonyl of Trp α 149,¹⁷ an interaction that had been anticipated by several modeling studies.^{15,16} To evaluate this possibility, the backbone amide at this position was converted to an ester by replacing Thr α 150 with the analog α -hydroxy threonine (Tah) using the nonsense suppression methodology (**Figure 2.6A**). Converting an amide carbonyl to an ester carbonyl weakens the hydrogen bonding ability of the oxygen. In studies of amide hydrogen bonds in the context of α -helices or β -sheets, the magnitude of the effect was 0.6 – 0.9 kcal/mol.^{41,42}

The results of the incorporation of Tah at $\alpha 150$ are shown in **Table 2.2**. Upon ester substitution, the EC_{50} for nicotine increases 1.6 fold. The change is larger for the more potent agonist epibatidine; conversion of the backbone carbonyl of Trp $\alpha 149$ to an ester leads to a 3.7-fold increase in EC_{50} (**Figure 2.6**). In contrast, ACh, lacking a proton at the cationic center, shows a 3.3 fold *decrease* in EC_{50} . These results further highlight the distinction between nicotinic and cholinergic agonists.

Table 2.2. Mutations Testing H-bond Interactions at $\alpha 150^a$

Agonist	Thr ^b	Tah	Tah/Thr
ACh	0.83 ± 0.04	0.25 ± 0.01	0.30
Nicotine	57 ± 2	92 ± 4	1.6
Epibatidine	0.60 ± 0.04	2.2 ± 0.2	3.7

^a EC_{50} (μM) \pm standard error of the mean.

The receptor has a Leu9'Ser mutation in M2 of the β subunit.

^b Rescue of wild type by nonsense suppression.

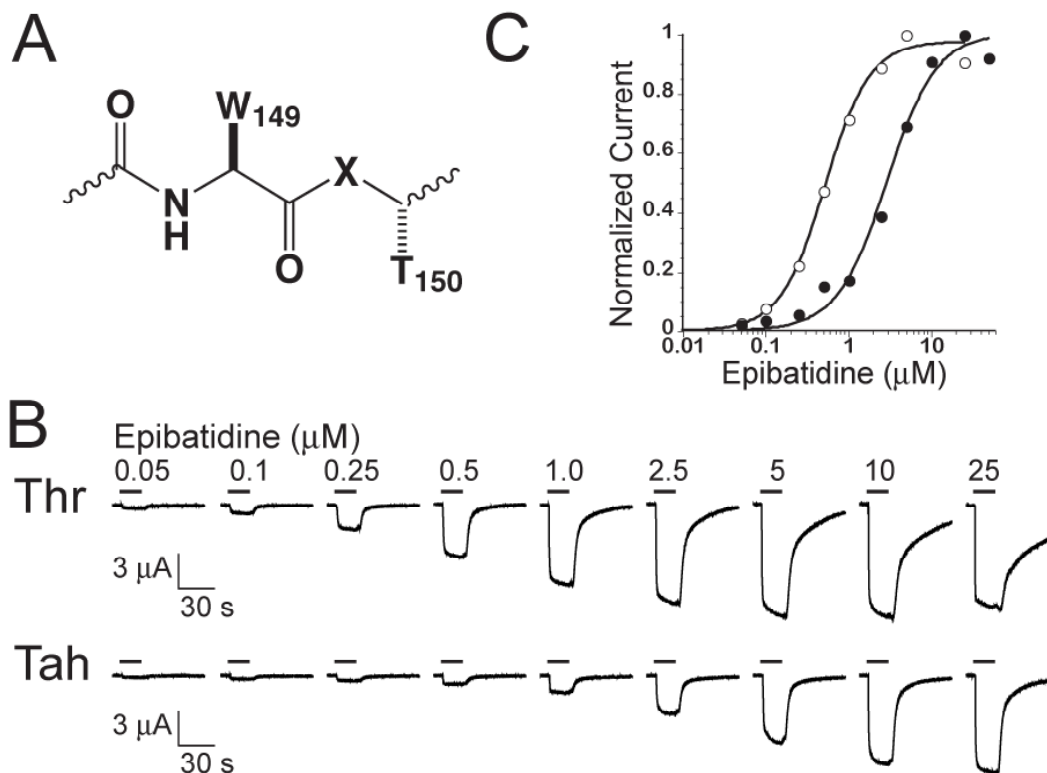


Figure 2.6. Hydrogen Bond Analysis of nAChR. (A) The backbone amide carbonyl of Trp α 149 ($X = \text{NH}$) is replaced with an ester carbonyl ($X = \text{O}$) upon incorporation of Tah α 150. (B) & (C) Electrophysiological analysis of epibatidine. (B) Representative voltage-clamp current traces for oocytes expressing nAChRs suppressed with Thr or Tah at α 150. Bars represent application of epibatidine at the concentrations noted. (C) Representative epibatidine dose-response relations and fits to the Hill equation for nAChR suppressed with Thr (\circ) and Tah (\bullet). Studies incorporate a β Leu9 \rightarrow Ser mutation.

Amide and Ester Efficacy at α 150

Agonist efficacy on a LGIC is measured by determining the maximal whole-cell current induced in response to saturating agonist concentrations. Full agonists maximally activate nAChR, while partial agonists sub-maximally activate the receptor resulting in a lower efficacy.⁴³ By comparing maximal currents induced by agonists on the same cell, partial agonists can be identified. The present study examines the maximal current in response to saturating doses, approximately three times the EC_{50} , of ACh, nicotine, and

epibatidine to probe agonist strength in the presence of the ester backbone mutation at $\alpha 150$ (**Figure 2.7**). Interestingly, nicotine and epibatidine efficacy decrease for the ester mutant in comparison to the wild-type amide backbone at position $\alpha 150$ to approximately 40% and 70%, respectively. Thus, nicotine appears to be a partial agonist for the ester mutant at $\alpha 150$.

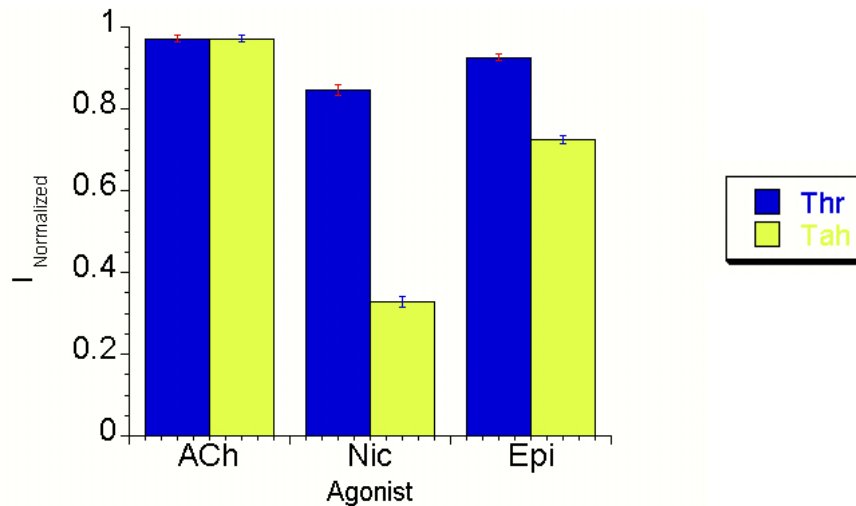


Figure 2.7. Agonist Efficacy Studies. Efficacy measurements for oocytes expressing nAChR suppressed with the indicated residue at $\alpha 150$ in response to saturating concentrations of the indicated agonist. The receptor has a Leu9'Ser mutation in M2 of the β subunit. Mean whole-cell currents were obtained and normalized to the maximal signal elicited for ACh; ACh is assumed to be a full agonist in each system. Normalized data were averaged and are reported along with the SEM. Concentrations of each agonist were ACh 0.75 μ M, nicotine 275 μ M, and epibatidine 6.5 μ M.

Events involving nAChR agonist binding and channel gating are complicated and are postulated to involve numerous steps. While the present study examines mutations in the binding site region, it is possible that these mutations affect channel gating as well as agonist binding. These results from the efficacy studies indicate that the processes observed in the Tah ester mutant might involve both binding and gating factors for

nicotine. Thus, future studies such as single channel kinetic experiments are necessary to further probe these observations.

Computational Modeling

In order to further probe the interactions of drugs with Trp α 149, a simple computational model was investigated. Considering only the interactions with Trp α 149, we docked the ligands using *ab initio* (HF/6-31G) calculations taking into account both the cation- π interaction and the carbonyl hydrogen bond. Initial tryptophan and ligand coordinates were taken from the AChBP-based homology models of Changeux.¹⁶ Geometry optimizations, counterpoise corrections, and zero point energy corrections were all performed in the gas phase. The optimized geometries for free ACh and nicotine are in keeping with previous calculations at higher levels of theory and with solution NMR studies, in that bent "tg" structures are favored for ACh and the *trans* form is favored for protonated nicotine.⁴⁴⁻⁴⁶ The calculated binding energies are consistent with those from previous computational studies of metal-binding complexes with both cation- π and cation-carbonyl interactions⁴⁷⁻⁵¹ and studies of hydrogen bonds to protonated nicotine.^{52,53}

The calculated binding energies are summarized in **Table 2.3** and described in more detail elsewhere.²⁹ As expected, conversion of the Trp α 149 amide to an ester weakens the binding interactions to both epibatidine and nicotine, and the calculated energetic consequence of ester conversion is larger for epibatidine than for nicotine (8 kcal/mol vs. 6 kcal/mol). Using the PCM solvation model,³³ we also studied these interactions in solvents of differing polarity (**Table 2.3**). In each solvent, epibatidine favors amide binding over ester binding to a greater degree than nicotine. The changes in hydrogen-

bonding energies observed in different solvent systems are consistent with similar calculations published by Houk and co-workers.⁵⁴

Table 2.3. Solvent Effects on Binding Energy Differences^a

Agonist	Ester Binding Energy –			
	Gas	THF	Ethanol	Water
ACh	5.0	0.6	- 1.7	- 2.0
Nicotine	6.1	3.1	1.2	- 0.8
Epibatidine ^b	8.0	7.0	5.0	4.7

^a $\epsilon(\text{THF}) = 7.6$, $\epsilon(\text{ethanol}) = 24.3$, $\epsilon(\text{water}) = 78.5$.

^b Average of energies for Epi enantiomers.

The geometries of **Figure 2.8** are consistent with the experimental trends observed. The cation- π interaction is expected to be much stronger for epibatidine than for nicotine. The calculated N^+ to π -centroid distance is substantially shorter for epibatidine (**a** in **Figure 8**). In addition, epibatidine points an $\text{N}^+\text{-H}$ cationic center towards the Trp indole ring vs. the $\text{N}^+\text{CH}_2\text{-H}$ of nicotine (**Figure 2.8**). The cationic center of epibatidine has a much more positive electrostatic potential than that of nicotine (+139 kcal/mol for epibatidine, +112 for nicotine). These potentials, indicators of cation- π binding strength, and the geometrical factors noted are consistent with the experimental observation that epibatidine has a much stronger cation- π interaction than nicotine.

Nicotine and epibatidine also make significant hydrogen bonds to the Trp α 149 carbonyl oxygen with an $\text{N}^+\text{-H}$ group (**b** in **Figure 2.8**). The geometrical parameters for interaction **b** with the two agonists are very similar, suggesting the two hydrogen bonds are comparably strong. In addition, the calculations suggest a second, previously

unanticipated interaction between the $C_{\text{aromatic}}\text{-H}$ of the carbon adjacent to the pyridine N of epibatidine and the same carbonyl (**c** in **Figure 2.8**). This type of $C\text{-H}\cdots\text{O}=\text{C}$ hydrogen bond has been seen in many protein structures and other systems, and the geometrical parameters of the epibatidine structures are compatible with previous examples.^{55,56} (+) Epibatidine has a calculated C-O distance (**c** in **Figure 2.8**) of 3.19 Å, and a C-H-O angle of 151°; (-) epibatidine has a longer C-O distance of 3.26 Å, but a more favorable angle, 169°. In the computed nicotine-bound structure, the analogous distances and angles are less favorable (**c** in **Figure 2.8**): 3.42 Å and 139°, and the interaction is completely absent in the x-ray structure.

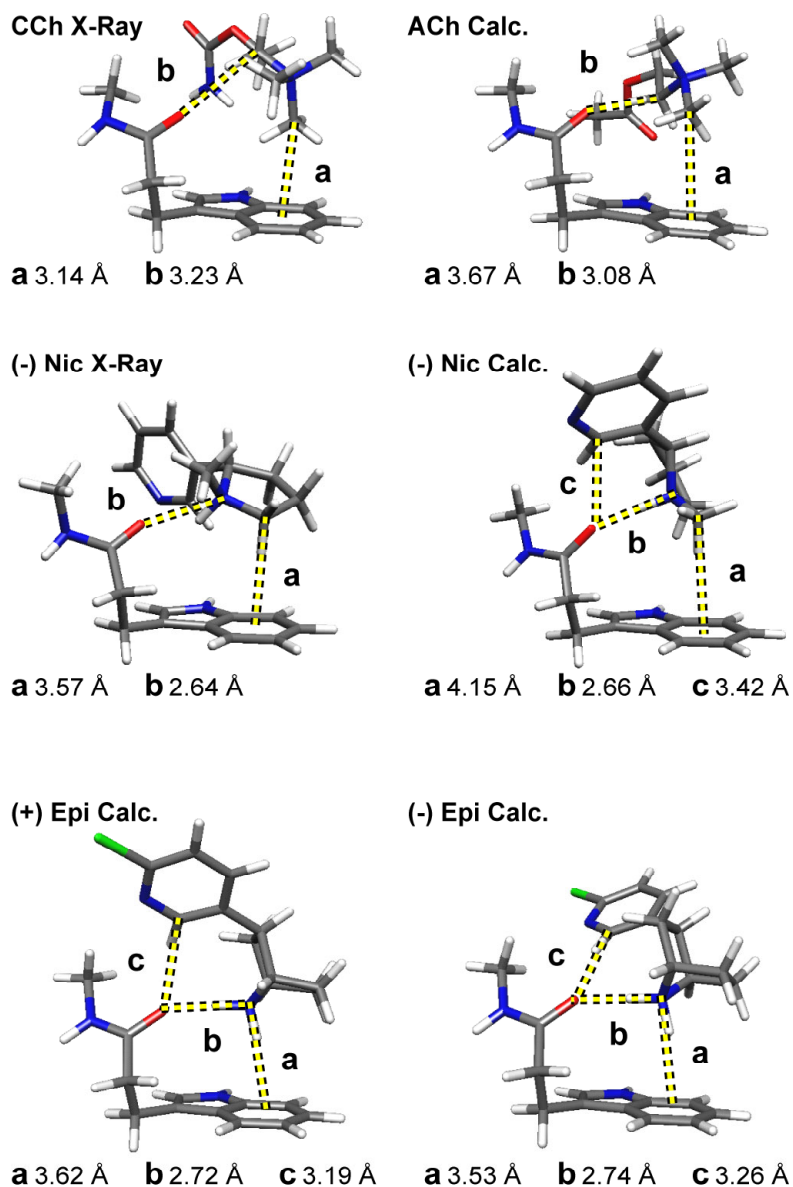


Figure 2.8. Crystal Structure Data (X-Ray) and Computational Modeling (Calc.) of Agonist Binding. Crystal structures for CCh and nicotine were taken from Celie *et al.* (PDB ID 1UW6 (nicotine) and 1UV6 (CCh)).¹⁷ Calculations were performed for ACh, (-) nicotine, (+) epibatidine, and (-) epibatidine. Distance **a** represents a cation- π interaction; **b** represents an N^+-H or N^+C-H hydrogen bond with the backbone carbonyl and **c** represents a $C_{aromatic}-H \cdots O=C$ hydrogen bond with the backbone carbonyl. Gas phase HF/6-31G optimized geometries (Å) are reported. Hydrogens were added to the x-ray structures using Gaussview.

2.4 DISCUSSION

A number of studies have identified key interactions that lead to the binding of small molecules at the agonist-binding site of nAChRs.⁵⁷ The field was dramatically altered with the appearance of the crystal structure of the ACh binding protein. AChBP is not the nAChR, however. It is a small, soluble protein secreted from the glial cells of a snail, and it is < 25% identical to its closest relative in the nAChR family, $\alpha 7$.⁹ It remains to be established just how relevant AChBP is to the functional receptors.⁵⁸ The methodology of incorporating unnatural amino acids into these receptors provides a functional tool to address this task.

Previously, we observed an intriguing result: nicotine and ACh use different noncovalent interactions to bind the muscle-type nAChR.¹⁴ ACh forms a strong cation- π interaction with Trp $\alpha 149$; nicotine does not. Although known as the nicotinic receptor, the form we study here, that found in the peripheral nervous system, is relatively insensitive to nicotine. At this muscle-type receptor ACh is over 70-fold more potent than nicotine. The behavioral and addictive effects of nicotine arise exclusively from interactions with one or more neuronal subtypes of nAChR found in the central nervous system, where nicotine and ACh are generally comparably potent. We therefore wanted to probe a nicotinic-type agonist that is potent at the muscle receptor, and epibatidine was the logical choice. This alkaloid natural product possesses potent analgesic properties⁵⁹ and has served as a lead compound for a number of pharmaceutical programs targeted at the nAChR.²² In the present work, we find two specific interactions that distinguish among the three agonists considered here, ACh, nicotine, and epibatidine.

First, we now find that epibatidine makes a strong cation- π interaction with Trp α 149 of the muscle-type nAChR. This result contrasts sharply to nicotine, and this observation helps to explain the much higher affinity of epibatidine for this receptor relative to nicotine. The apparent magnitudes of the cation- π interactions, indicated by the slopes of the fluorination plots in **Figure 2.4**, are comparable for ACh and epibatidine. This similarity is somewhat surprising. It is well established that quaternary ammonium cations make weaker cation- π interactions than protonated ammoniums (be they primary, secondary, or tertiary), and the electrostatic model of the cation- π interaction nicely rationalizes this effect.^{10,11,60} In addition, we have shown that when serotonin is the agonist binding to a Trp in two different receptors, a steeper slope for the fluorination plot is seen than that for ACh in the nAChR.^{14,39} Serotonin contains a primary ammonium ion, and so the steeper slope is considered to be consistent with the expected stronger cation- π interaction. We conclude that epibatidine makes a strong cation- π interaction-comparable to that for ACh—but that, at least at the muscle receptor, it cannot maximize its binding to the indole ring of Trp α 149 due to other binding constraints.

The second discriminator we have probed is hydrogen bonding. A newer crystal structure of the AChBP includes nicotine at the binding site.¹⁷ The structure confirms the existence of a hydrogen bond between nicotine and the backbone carbonyl of Trp α 149, an interaction anticipated by modeling studies. In efforts to probe this non-covalent interaction, we studied the effects of decreasing the hydrogen bond acceptor ability of the backbone carbonyl of Trp α 149. In such studies, the clear distinction between ACh and nicotinic agonists is strengthened. Nicotine and epibatidine, containing a tertiary and secondary cationic center, respectively, both show increases in EC_{50} compared to the native receptor in response to the amide-to-ester modification (**Table 2.2**). The effect is

larger with the more potent agonist, epibatidine. Thus, the experimental data support the suggestion that nicotine and epibatidine interact with the nAChR through a hydrogen bond with the backbone carbonyl of Trp α 149.

ACh, with a quaternary cationic center that cannot make a conventional hydrogen bond, shows a decrease in EC_{50} at the ester-containing receptor compared to the native receptor. We had anticipated that the binding of ACh would be unaffected by such a subtle change. The origin of this effect is unclear from these studies and is further investigated in Chapter 3. Here we consider two possibilities.

In the recently reported crystal structure of AChBP binding to carbamylcholine (CCh),¹⁷ a cholinergic analogue of ACh, the backbone carbonyl oxygen of interest here makes contact with a CH_2 group adjacent to the $N^+(CH_3)_3$ group (CCh: $NH_2C(O)OCH_2CH_2N^+(CH_3)_3$). This CH_2 carries a significant positive charge, like the CH_3 groups, and so a favorable electrostatic interaction is possible. This interaction with CCh would be much weaker than the $N^+ \cdots H$ hydrogen bonds of nicotine and epibatidine, but perhaps not negligible. Interestingly, Sixma and co-workers noted that the binding of CCh to AChBP is less enthalpically favorable than that of nicotine. They attribute this observation to the net unfavorable burial of the carbonyl oxygen by CCh. The weak interaction with the CH_2 group cannot compensate for the loss of hydrogen bonding, presumably to water molecules. This desolvation penalty would be less severe with a backbone ester rather than an amide, so ACh binds more favorably to the ester-containing receptor.

We also propose a second possible explanation. Highly conserved Asp α 89 (Asp 85 in AChBP numbering) makes a number of significant contacts with nearby residues, suggesting it plays a key structural role in shaping the agonist-binding site.^{9,17} One such

interaction is a hydrogen bond between the Asp α 89 carboxylate side chain and the NH group of the backbone amide of Trp α 149. The amide-to-ester mutation of the present study eliminates the NH and so removes this interaction. A possible outcome of this alteration could be a structural change that would affect gating, biasing the conformational change in the direction of the open channel. A gating effect of this sort could be revealed by single-channel kinetic analyses, and future studies are necessary.

Regardless of its origin, it is reasonable to propose that the effect of ester substitution we see with ACh can be considered as the “background” for the Thr150Tah mutation. That is, if the magnitude of the cholinergic $N^+CH_2\cdots O=C$ interaction is small, then both the desolvation and gating effects proposed are “generic” and should occur with all agonists. In this case, the changes in EC_{50} we measure for nicotine or epibatidine actually represent the product of two terms: a generic 3.3-fold decrease evidenced by ACh, and a term specific to nicotine or epibatidine. As such, the drop in hydrogen-bonding strength is calculated to be 1.6×3.3 or ~ 5 -fold for nicotine, and 3.7×3.3 or ~ 12 -fold for epibatidine. Energetically, these factors correspond to 1.0 and 1.5 kcal/mol, respectively. This is the first experimental evaluation of a hydrogen-bonding interaction between a protein backbone and a ligand using backbone ester substitution. The magnitude we see is larger than what has been reported for amide \cdots amide hydrogen bonds that stabilize protein secondary structure.^{41,42} Context is always important in such effects, so it is not surprising to see a difference between a ligand \cdots backbone interaction and a backbone \cdots backbone interaction. In addition, the hydrogen bond donor in the present system is cationic, as opposed to the neutral amide NH in the secondary structure studies. Hydrogen bonding involving ionic species is often stronger than for neutral species, and so our values seem quite reasonable.

Our experimental studies suggested that the two structurally quite similar molecules, nicotine and epibatidine, bind differently to the nAChR. Epibatidine experiences both a cation- π interaction and a backbone interaction with Trp α 149, while nicotine experiences only the latter. In an effort to shed some light on this issue, we performed appropriately simple calculations in which we docked both drugs onto Trp α 149. The goal here was not to obtain quantitative binding information. There are no doubt many other side chains that also contribute to the binding of these drugs, and, despite the AChBP structure, it is a substantial challenge to know how to evaluate these interactions. Our calculated ACh binding geometry in **Figure 2.8** agrees surprisingly well with the CCh crystal structure. The calculated geometry for nicotine, however, deviates from both the x-ray structure of nicotine bound to AChBP¹⁷ and the docked homology models of Changeux and co-workers.¹⁶ The nicotine geometry in **Figure 2.8** is obtained in HF/6-31G minimizations starting from either the docked coordinates of Le Novère *et al.* or the position of bound nicotine in the AChBP crystal structure. The fact that the relationship of nicotine to Trp α 149 changes upon minimization implies that other side chains are necessary to hold nicotine in the crystal structure orientation. Nevertheless, because the goal of our computational studies was to supplement our experimental results, these simple gas phase geometry optimizations are informative.

Remarkably, the relatively simple model calculations we have conducted afford trends that nicely parallel our experimental findings. One key test of the calculations arises from the fact that, experimentally, the EC_{50s} of (+) and (-) epibatidine are nearly identical for a given acetylcholine receptor subtype.⁵⁹ We find that the calculated binding energies to Trp α 149 and the key geometrical parameters (**Figure 2.8**) are indeed very similar for the two enantiomers.

In the gas phase, it is better to bind to the backbone amide than the ester for all three agonists. However, as solvation is introduced, the trend is reversed (**Table 2.3**). Interestingly, when a solvent of moderate polarity—ethanol—is used, ACh prefers the ester backbone, while nicotine and epibatidine prefer the amide, just as we see in our experimental studies. The ethanol environment is defined in these calculations by a dielectric constant of 24.3. Two lines of evidence indicate that this is a reasonable estimate of the effective dielectric of the binding pocket of the AChBP or nAChR. First, it is consistent with previous experimental measurements of a perturbed local pK_a in the nAChR binding site.⁴⁰ Second, calculations of the solvent accessible surface area (See reference²⁹) of the binding site residues show that Trp 149 is 11 % solvent-accessible. A moderate dielectric of 24.3 seems reasonable for the partially-exposed binding site. Thus, it may be, as discussed above, that the EC_{50} for ACh decreases when the ester is introduced because the desolvation penalty of the ester carbonyl oxygen is less severe than the amide.

The computer modeling summarized in **Figure 2.8** also nicely rationalizes the observed cation- π binding behavior. Epibatidine, like ACh, makes much closer contact with the indole ring than does nicotine. Both the distance (**a** in **Figure 2.8**) and the electrostatic potential on the interacting hydrogen (**Figure 2**: N^+H in epibatidine vs. N^+CH_2H in nicotine) suggest a more favorable cation- π interaction for epibatidine than for nicotine.

The larger amide/ester effect seen for epibatidine versus nicotine suggests a stronger $N^+H\cdots O=C$ hydrogen bond in the former. However, in the docked structures these hydrogen bonds (**b** in **Figure 2.8**) are geometrically very similar for epibatidine and nicotine, suggesting that they are of comparable strengths. The docking studies do,

however, suggest an alternative explanation. The docked epibatidine structure clearly shows a $C_{\text{aromatic}}-\text{H}\cdots\text{O}=\text{C}$ hydrogen bond from the drug to the backbone carbonyl. C-H \cdots O hydrogen bonds are well known, if structural features create a significant partial positive charge on the hydrogen.^{55,56} The $C_{\text{aromatic}}-\text{H}$ hydrogen bond of interest should be highly polarized to favor a hydrogen bond, because it is *ortho* to a pyridine nitrogen and *meta* to a chlorine substituent. Geometrically, the $C_{\text{aromatic}}-\text{H}$ hydrogen bond to the carbonyl (**c** in **Figure 2.8**) is tighter and better aligned for both epibatidine enantiomers than for nicotine. The computations thus suggest that it is this unconventional hydrogen bond (**c**), rather than the anticipated hydrogen bond (**b**), that rationalizes the slightly greater response of epibatidine versus nicotine to the backbone change. Note that the small structural differences between epibatidine and nicotine nicely rationalize their differing affinities. The secondary ammonium of epibatidine provides two N^+-H s that can undergo strong electrostatic interactions—a cation- π interaction and a hydrogen bond to a carbonyl. The tertiary ammonium of nicotine allows a strong hydrogen bond, but not a significant cation- π interaction. Second, the slightly different positioning of the pyridine group in epibatidine allows for a more favorable $C_{\text{aromatic}}-\text{H}\cdots\text{O}=\text{C}$ hydrogen bond than for nicotine.

The ability to systematically modify receptor structure enables studies of drug-receptor interactions with unprecedented precision. In other work we have established that a single drug, serotonin, can adopt two different binding orientations at highly homologous serotonin receptors.³⁹ Here we show that two agonists binding to the same binding site can make use of quite different noncovalent binding interactions to activate the receptor, even if the agonists are structurally very similar. No doubt medicinal chemists have anticipated such a result for some time, but it is only with the high

precision, physical chemistry tools described here that such possibilities can be directly addressed.

In summary, a combination of unnatural amino acid mutagenesis and computer modeling has led to the following conclusions. The nicotinic agonists nicotine and epibatidine both experience a favorable hydrogen-bonding interaction with the carbonyl of Trp α 149, which is qualitatively distinct from the interaction (if any) of ACh with this group. The greater potency of epibatidine relative to nicotine arises from the fact that, along with hydrogen bonding, epibatidine experiences a cation- π interaction comparable to that seen with ACh. In addition, epibatidine picks up a subtle $C_{\text{aromatic}}-\text{H}\cdots\text{O}=\text{C}$ hydrogen bond that nicotine does not.

At the neuronal nAChR both epibatidine and nicotine show much higher affinities than at the muscle type studied here, although epibatidine remains the more potent agonist across all receptor types. This suggests that the differentiating cation- π interaction seen here may carry over to the more pharmacologically relevant neuronal receptors. Additional studies along these lines are underway.

2.5 REFERENCES

1. Beene, D. L., Dougherty, D. A. & Lester, H. A. Unnatural amino acid mutagenesis in mapping ion channel function. *Current Opinion in Neurobiology* **13**, 264-70 (2003).
2. Dougherty, D. A. Unnatural amino acids as probes of protein structure and function. *Current Opinion in Chemical Biology* **4**, 645-652 (2000).
3. Cassels, B. K., Bermudez, I., Dajas, F., Abin-Carriquiry, J. A. & Wonnacott, S. From ligand design to therapeutic efficacy: the challenge for nicotinic receptor research. *Drug Discovery Today*, 1657-1665.
4. Paterson, D. & Nordberg, A. Neuronal nicotinic receptors in the human brain. *Progress in Neurobiology* **61**, 75-111 (2000).
5. Miyazawa, A., Fujiyoshi, Y., Stowell, M. & Unwin, N. Nicotinic acetylcholine receptor at 4.6 Å resolution: transverse tunnels in the channel wall. *Journal of Molecular Biology* **288**, 765-86 (1999).
6. Grutter, T. & Changeux, J. P. Nicotinic receptors in wonderland. *Trends in Biochemical Sciences* **26**, 459-463 (2001).
7. Karlin, A. Emerging structure of the nicotinic acetylcholine receptors. *Nature Reviews Neuroscience* **3**, 102-14 (2002).
8. Corringer, P.-J., Le Novère, N. & Changeux, J.-P. Nicotinic Receptors at the Amino Acid Level. *Annu. Rev. Pharmacol. Toxicol.* **40**, 431-458 (2000).
9. Brejc, K. et al. Crystal structure of an ACh-binding protein reveals the ligand-binding domain of nicotinic receptors. *Nature* **411**, 269-76 (2001).
10. Dougherty, D. A. Cation- π interactions in chemistry and biology: a new view of benzene, Phe, Tyr, and Trp. *Science* **271**, 163-8 (1996).
11. Ma, J. C. & Dougherty, D. A. The cation- π interaction. *Chemical Reviews* **97**, 1303-1324 (1997).
12. Zacharias, N. & Dougherty, D. A. Cation- π interactions in ligand recognition and catalysis. *Trends in Pharmacological Sciences* **23**, 281-287 (2002).
13. Zhong, W. et al. From ab initio quantum mechanics to molecular neurobiology: a cation- π binding site in the nicotinic receptor. *Proceedings of the National Academy of Sciences U S A* **95**, 12088-93 (1998).
14. Beene, D. L. et al. Cation- π interactions in ligand recognition by serotonergic (5-HT_{3A}) and nicotinic acetylcholine receptors: the anomalous binding properties of nicotine. *Biochemistry* **41**, 10262-9 (2002).
15. Schapira, M., Abagyan, R. & Totrov, M. Structural model of nicotinic acetylcholine receptor isotypes bound to acetylcholine and nicotine. *BioMed Central Structural Biology* **2**, 1 (2002).
16. Le Novère, N., Grutter, T. & Changeux, J. P. Models of the extracellular domain of the nicotinic receptors and of agonist- and Ca²⁺-binding sites. *Proceedings of the National Academy of Sciences of the United States of America* **99**, 3210-3215 (2002).
17. Celie, P. H. N. et al. Nicotine and Carbamylcholine Binding to Nicotinic Acetylcholine Receptors as Studied in AChBP Crystal Structures. *Neuron* **41**, 907-914 (2004).

18. Akk, G. & Auerbach, A. Activation of muscle nicotinic acetylcholine receptor channels by nicotinic and muscarinic agonists. *British Journal of Pharmacology* **128**, 1467-76 (1999).
19. Gerzanich, V. et al. Comparative pharmacology of epibatidine: a potent agonist for neuronal nicotinic acetylcholine receptors. *Molecular Pharmacology* **48**, 774-82 (1995).
20. Prince, R. J. & Sine, S. M. Epibatidine activates muscle acetylcholine receptors with unique site selectivity. *Biophysical Journal* **75**, 1817-27 (1998).
21. Badio, B. & Daly, J. W. Epibatidine, a potent analgetic and nicotinic agonist. *Molecular Pharmacology* **45**, 563-9 (1994).
22. Dukat, M. & Glennon, R. A. Epibatidine: impact on nicotinic receptor research. *Cellular and Molecular Neurobiology* **23**, 365-78 (2003).
23. Servi, S. 2,2,5-Trimethyl-1,3-Dioxolane-4-Carboxaldehyde as a Chiral Synthone - Synthesis of the 2 Enantiomers of Methyl 2,3,6-Trideoxy-Alpha-L-Threo-Hex-2-Enopyranoside, Key Intermediate in the Synthesis of Daunocamine, and of (+)- and (-)-Rhodinose. *Journal of Organic Chemistry* **50**, 5865-5867 (1985).
24. England, P. M., Lester, H. A. & Dougherty, D. A. Incorporation of esters into proteins: Improved synthesis of hydroxyacyl tRNAs. *Tetrahedron Letters* **40**, 6189-6192 (1999).
25. England, P. M., Zhang, Y. N., Dougherty, D. A. & Lester, H. A. Backbone mutations in transmembrane domains of a ligand-gated ion channel: Implications for the mechanism of gating. *Cell*, 89-98.
26. Zacharias, N. in *Chemistry* (Caltech, Pasadena, 2004).
27. Nowak, M. W. et al. In vivo incorporation of unnatural amino acids into ion channels in *Xenopus* oocyte expression system. *Ion Channels, Pt B* **293**, 504-529 (1998).
28. Li, L. T. et al. The tethered agonist approach to mapping ion channel proteins toward a structural model for the agonist-binding site of the nicotinic acetylcholine receptor. *Chemistry & Biology* **8**, 47-58 (2001).
29. Cashin, A. L., Petersson, E. J., Lester, H. A. & Dougherty, D. A. Using physical chemistry to differentiate nicotinic from cholinergic agonists at the nicotinic acetylcholine receptor. *Journal of the American Chemical Society* **127**, 350-356 (2005).
30. Boys, S. F. & Bernardi, F. Calculation of Small Molecular Interactions by Differences of Separate Total Energies-Some Procedures with Reduced Errors. *Molecular Physics* **19**, 553-& (1970).
31. Foresman, J. B. & Frisch, E. *Exploring Chemistry with Electronic Structure Methods* (Gaussian, Inc., Pittsburgh, PA, 1996).
32. Frisch, M. J. et al. (Gaussian, Inc., Pittsburgh PA, 1998).
33. Cossi, M., Barone, V., Cammi, R. & Tomasi, J. Ab initio study of solvated molecules: A new implementation of the polarizable continuum model. *Chemical Physics Letters* **255**, 327-335 (1996).
34. Flükiger, P., Lüthi, H. P., Portmann, S. & Weber, J. (Swiss Center for Scientific Computing, Manno, Switzerland, 2000).
35. Filatov, G. N. & White, M. M. The role of conserved leucines in the M2 domain of the acetylcholine receptor in channel gating. *Mol Pharmacol* **48**, 379-84 (1995).

36. Revah, F., Bertrand, D., Galzi, J. L., Devillers-Theiry, A. & Mulle, C. Mutations in the channel domain alter desensitization of a neuronal nicotinic receptor. *Nature* **353**, 846-849 (1991).
37. Labarca, C. et al. Channel gating governed symmetrically by conserved leucine residues in the M2 domain of nicotinic receptors. *Nature* **376**, 514-516 (1995).
38. Kearney, P. C. et al. Agonist binding site of the nicotinic acetylcholine receptor: Tests with novel side chains and with several agonists. *Molecular Pharmacology* **50**, 1401-1412 (1996).
39. Mu, T. W., Lester, H. A. & Dougherty, D. A. Different binding orientations for the same agonist at homologous receptors: A lock and key or a simple wedge? *Journal of the American Chemical Society* **125**, 6850-6851 (2003).
40. Petersson, E. J., Choi, A., Dahan, D. S., Lester, H. A. & Dougherty, D. A. A perturbed pK(a) at the binding site of the nicotinic acetylcholine receptor: implications for nicotine binding. *Journal of the American Chemical Society* **124**, 12662-3 (2002).
41. Deechongkit, S. et al. Context-dependent contributions of backbone hydrogen bonding to beta-sheet folding energetics. *Nature* **430**, 101-5 (2004).
42. Koh, J. T., Cornish, V. W. & Schultz, P. G. An experimental approach to evaluating the role of backbone interactions in proteins using unnatural amino acid mutagenesis. *Biochemistry* **36**, 11314-22 (1997).
43. Kenakin, T. Efficacy at G-protein-coupled receptors. *Nature Reviews Drug Discovery* **1**, 103-10 (2002).
44. Elmore, D. E. & Dougherty, D. A. A computational study of nicotine conformations in the gas phase and in water. *Journal of Organic Chemistry* **65**, 742-747 (2000).
45. Vistoli, G., Pedretti, A., Villa, L. & Testa, B. The solute-solvent system: solvent constraints on the conformational dynamics of acetylcholine. *Journal of the American Chemical Society* **124**, 7472-80 (2002).
46. Partington, P., Feeney, J. & Burgen, A. S. The conformation of acetylcholine and related compounds in aqueous solution as studied by nuclear magnetic resonance spectroscopy. *Molecular Pharmacology* **8**, 269-77 (1972).
47. Biot, C., Buisine, E. & Rooman, M. Free-energy calculations of protein-ligand cation-pi and amino-pi interactions: From vacuum to proteinlike environments. *Journal of the American Chemical Society* **125**, 13988-13994 (2003).
48. Biot, C., Wintjens, R. & Rooman, M. Stair motifs at protein-DNA interfaces: Nonadditivity of H-bond, stacking, and cation-pi interactions. *Journal of the American Chemical Society* **126**, 6220-6221 (2004).
49. Sponer, J. E., Sychrovsky, V., Hobza, P. & Sponer, J. Interactions of hydrated divalent metal cations with nucleic acid bases. How to relate the gas phase data to solution situation and binding selectivity in nucleic acids. *Physical Chemistry Chemical Physics* **6**, 2772-2780 (2004).
50. Sponer, J., Leszczynski, J. & Hobza, P. Electronic properties, hydrogen bonding, stacking, and cation binding of DNA and RNA bases. *Biopolymers* **61**, 3-31 (2001).
51. Siu, F. M., Ma, N. L. & Tsang, C. W. Competition between π and Non- π Cation-Binding Sites in Aromatic Amino Acids: A Theoretical Study of Alkali Metal

- Cation (Li^+ , Na^+ , K^+)-Phenylalanine Complexes. *Chemistry-A European Journal* **10**, 1966-1976 (2004).
52. Graton, J. et al. The nicotinic pharmacophore: Thermodynamics of the hydrogen-bonding complexation of nicotine, normicotine, and models. *Journal of Organic Chemistry* **68**, 8208-8221 (2003).
 53. Graton, J., van Mourik, T. & Price, S. L. Interference between the hydrogen bonds to the two rings of nicotine. *Journal of the American Chemical Society* **125**, 5988-97 (2003).
 54. Cannizzaro, C. E. & Houk, K. N. Magnitudes and chemical consequences of $\text{R(3)N(+)C-H}\dots\text{O[double bond]C}$ hydrogen bonding. *Journal of the American Chemical Society* **124**, 7163-9 (2002).
 55. Thomas, K. A., Smith, G. M., Thomas, T. B. & Feldmann, R. J. Electronic distributions within protein phenylalanine aromatic rings are reflected by the three-dimensional oxygen atom environments. *Proc Natl Acad Sci U S A* **79**, 4843-7 (1982).
 56. Duan, G., Smith, V. H. & Weaver, D. F. Characterization of Aromatic-Amide(Side-Chain) Interactions in Proteins through Systematic ab Initio Calculations and Data Mining Analyses. *J. Phys. Chem. A* **104**, 4521-4532 (2000).
 57. Schmitt, J. D. Exploring the nature of molecular recognition in nicotinic acetylcholine receptors. *Current Medicinal Chemistry* **7**, 749-800 (2000).
 58. Bouzat, C. et al. Coupling of agonist binding to channel gating in an ACh-binding protein linked to an ion channel. *Nature* **430**, 896-900 (2004).
 59. Spande, T. F. et al. Epibatidine-a Novel (Chloropyridyl)Azabicycloheptane with Potent Analgesic Activity from an Ecuadorian Poison Frog. *Journal of the American Chemical Society* **114**, 3475-3478 (1992).
 60. Mecozzi, S., West, A. P. & Dougherty, D. A. Cation- Π Interactions in Simple Aromatics: Electrostatics Provide a Predictive Tool. *J. Am. Chem. Soc.* **118**, 2307-2308 (1996).